JVSTA
JOURNAL OF VACUUM SCIENCE AND TECHNOLOGY A

Luminescence enhancement of plasma-etched InAsP/InGaAsP quantum wells

Meng Cao, Yanfeng Lao, Huizhen Wu, Cheng Liu, Zhengsheng Xie et al.

Citation: J. Vac. Sci. Technol. A **26**, 219 (2008); doi: 10.1116/1.2831497
View online: http://dx.doi.org/10.1116/1.2831497
View Table of Contents: http://avspublications.org/resource/1/JVTAD6/v26/i2
Published by the AVS: Science & Technology of Materials, Interfaces, and Processing

Related Articles

Blueshift in sulfur treated GaAsP/AlGaAs near surface quantum well
J. Vac. Sci. Technol. A 30, 021401 (2012)

Room temperature capacitance-voltage profile and photoluminescence for delta doped InGaAs single quantum well
J. Vac. Sci. Technol. B 28, C3I6 (2010)

Optical study of ZnO/ZnMgO quantum wells grown by metal organic vapor phase epitaxy on ZnO substrates
J. Vac. Sci. Technol. B 27, 1755 (2009)

Electronic band gap of Si/SiO2 quantum wells: Comparison of ab initio calculations and photoluminescence measurements
J. Vac. Sci. Technol. A 25, 1500 (2007)

Radiative and nonradiative lifetimes in nonpolar m-plane InxGa1−xN/GaN multiple quantum wells grown on GaN templates prepared by lateral epitaxial overgrowth
J. Vac. Sci. Technol. B 25, 1524 (2007)

Additional information on J. Vac. Sci. Technol. A

Journal Homepage: http://avspublications.org/jvsta
Journal Information: http://avspublications.org/jvsta/about/about_the_journal
Top downloads: http://avspublications.org/jvsta/top_20_most_downloaded
Information for Authors: http://avspublications.org/jvsta/authors/information_for_contributors

ADVERTISEMENT

Luminescence enhancement of plasma-etched InAsP/InGaAsP quantum wells

Meng Cao,[a] Yanfeng Lao, Huizhen Wu, Cheng Liu, Zhengsheng Xie, and Chunfang Cao
State Key Laboratory of Functional Materials for Informatics, Shanghai Institute of Microsystem and Information Technology, Chinese Academy of Sciences, 865 Changning Road, Shanghai 200050, China

Huizhen Wu[b]
Department of Physics, Zhejiang University, Hangzhou, Zhejiang 310027, China

(Received 9 April 2007; accepted 10 December 2007; published 22 January 2008)

Luminescence enhancement effects are observed in the plasma-etched $InAs_{0.45}P_{0.55}/In_{0.68}Ga_{0.32}As_{0.45}P_{0.55}$ quantum wells (QWs). Characterizations of photoluminescence, atomic force microscopy, and secondary-ion mass spectroscopy reveal that surface roughening due to ion bombardment onto surface and microstructure changes resulted from Ar^+ ions tunneling into the material in the plasma etching process account for the PL enhancement phenomenon. The combination of plasma etching and selective lift-off of the InP cap layer of the $InAs_{0.45}P_{0.55}/In_{0.68}Ga_{0.32}As_{0.45}P_{0.55}$ QW structures allows us to separate the two enhancement factors, which indicates the Ar^+ ions tunneling into the crystal is the dominant factor that enhances the luminescence emission of $InAs_{0.45}P_{0.55}/In_{0.68}Ga_{0.32}As_{0.45}P_{0.55}$ quantum wells. © *2008 American Vacuum Society.* [DOI: 10.1116/1.2831497]

I. INTRODUCTION

In recent years, plasma etching, such as reactive-ion etching (RIE) and inductively coupled plasma (ICP), has been widely used for pattern transfer in fabricating III-V semiconductor devices due to its superior uniformity, controllability, and lower cost.[1,2] However, plasma etching may damage the semiconductor crystal, which degrades the optical and electrical performance of the semiconductor devices.[3–6] However, a few papers reported on the observation of enhanced photoluminescence (PL) emission from quantum well (QW) structures that were plasma etched though no comprehensive explanations were given for this phenomenon.[7] These controversial reports let us explore the PL enhancement mechanism of plasma-etched QWs.

InAsP/InGaAsP QWs have been widely used as active-region materials for optoelectronic devices in the 0.9–1.5 μm wavelength range, such as lasers and modulators.[8–10] Plasma etching is used extensively in fabricating InAsP/InGaAsP QW optoelectronic devices. In this article, we report the observation of significant enhancement of PL of plasma-etched InAsP/InGaAsP QWs. The mechanism of the enhancement is analyzed by the combination of PL, atomic force microscopy (AFM), and secondary-ion mass spectrometry (SIMS) to characterize the changes in surface morphology and microstructure after plasma etching. Surface roughening and Ar^+ ions tunneling into the crystal in the plasma-etched samples are two factors that contribute to the enhancement of PL emission.

II. EXPERIMENTS

Two QW structures of $InAs_{0.45}P_{0.55}/In_{0.68}Ga_{0.32}As_{0.45}P_{0.55}$ were grown on InP(100) substrates by gas-source molecule-beam epitaxy (GSMBE): an $InAs_{0.45}P_{0.55}/In_{0.68}Ga_{0.32}As_{0.45}P_{0.55}$ single quantum-well (SQW) structure and an $InAs_{0.45}P_{0.55}/In_{0.68}Ga_{0.32}As_{0.45}P_{0.55}$ multiple quantum-well (MQW) structure with varied well width. For the SQW structure, the $InAs_{0.45}P_{0.55}$ well width is 9 nm and the two $In_{0.68}Ga_{0.32}As_{0.45}P_{0.55}$ barriers are both 10 nm thick. The SQW is capped with a 50-nm-thick InP layer. The MQW structure consists of six $InAs_{0.45}P_{0.55}$ wells with varied well width (from bottom to top): 9.6, 6.6, 5.0, 4.0, 3.2, and 2.4 nm. The barriers are all 30-nm-thick $In_{0.68}Ga_{0.32}As_{0.45}P_{0.55}$, and the cap layer of the MQWs is 80-nm-thick InP.

Before plasma etching, a 420-nm-thick SiN_x layer was deposited on half of the sample surfaces by plasma-enhanced chemical-vapor deposition. The samples were then etched to different depths by ICP. The etching gases used in ICP were Cl_2 and Ar with flow rates of 6 and 12 SCCM (SCCM denotes cubic centimeter per minute at STP), respectively. A low ICP power (200 W) was adopted, and the self-bias was 130 V. After plasma etching, SiN_x was removed by HF solution. Etching depth was measured by a Talystep (XP-2) profiler. All of the PL measurements were done at room temperature by using the 514.5 nm excitation line of an Ar^+ ion laser with pumping power density of 13 W/cm^2.

III. RESULTS AND DISCUSSION

A. Observation of PL enhancement by plasma etching

Figure 1 shows the PL spectra of the as-grown and the plasma-etched $InAs_{0.45}P_{0.55}/In_{0.68}Ga_{0.32}As_{0.45}P$ MQWs. For the as-grown sample, the six PL peaks shown in spectrum (a) correspond to the quantum transitions from the first electronic subband to the first heavy hole subband (E1-HH1) of six wells with different well widths. After plasma etching of

[a]Electronic mail: cm2004@mail.sim.ac.cn
[b]Electronic mail: hzwu@zju.edu.cn

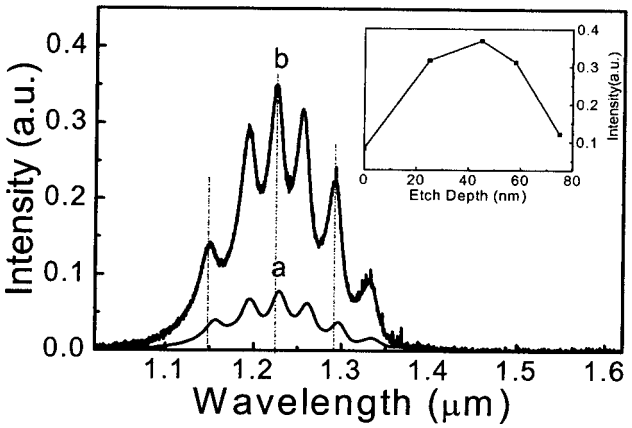

FIG. 1. PL intensity of $InAs_{0.45}P_{0.55}/InGa_{0.32}As_{0.45}P_{0.55}$ MQWs: (a) as-grown sample; (b) plasma-etched 45 nm sample. In the inset is the PL intensity of well 3 vs etching depth.

the MQW sample, all the six PL peaks display blueshift (about a few nanometers) relative to the as-grown sample which is shown in spectrum (b). This small blueshift could be attributed to the well/barrier disordering. The inset of Fig. 1 plots the PL intensity of the third well versus etching depth. It can be seen from Fig. 1 that the variation of PL intensity of the third well versus etching depth represents the PL intensity variation of all six wells. From the inset, it can be seen that as the etching depth increases, the PL intensity enhances quickly. When the etching depth reaches 45 nm the PL enhancement is at maximum and it is about four times of the PL intensity of the as-grown sample. However, as the etching depth continues to increase the PL intensity decreases gradually.

Figure 2 shows the measured PL spectra of four $InAs_{0.45}P_{0.55}/InGa_{0.32}As_{0.45}P_{0.55}$ SQW samples: (a) as-grown one; (b) plasma-etched 20 nm; (c) wet etched 30 nm after plasma etching of 20 nm; (d) directly wet-etched 50 nm. Here, a selectively wet etching method was used to lift off InP capping layer in samples (c) and (d) and the selective etching solution was $HCl:H_3PO_4$ (1:3). As seen in Fig. 2,

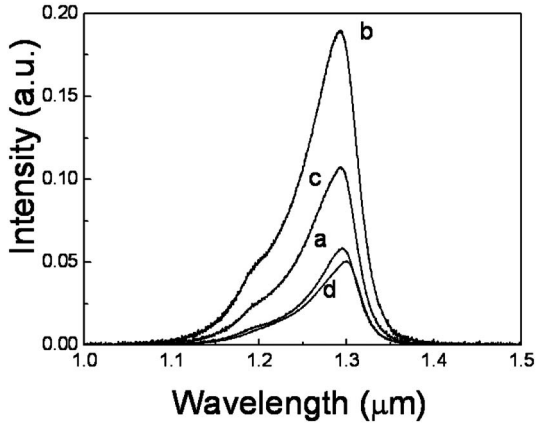

FIG. 2. PL spectra of $InAs_{0.45}P_{0.55}/InGa_{0.32}As_{0.45}P_{0.55}$ SQW: (a) as-grown sample; (b) plasma-etched 20 nm sample; (c) wet-etched 30 nm after plasma-etched 20 nm sample; (d) directly wet-etched 50 nm sample.

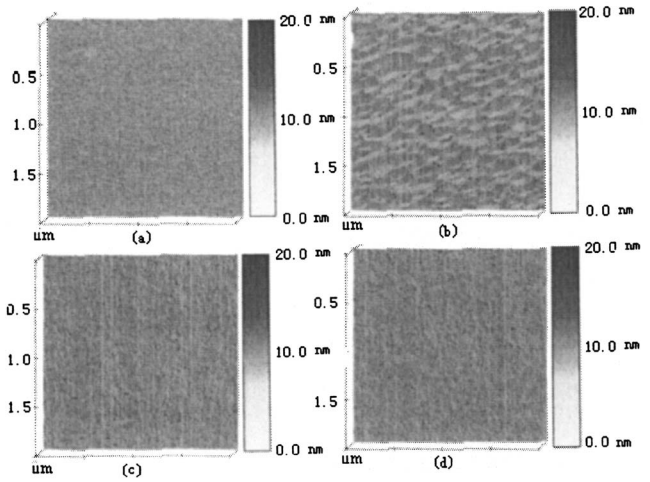

FIG. 3. AFM images of $InAs_{0.45}P_{0.55}/InGa_{0.32}As_{0.45}P_{0.55}$ SQW: (a) as-grown sample; (b) etched 20 nm sample; (c) wet-etched 30 nm after plasma-etched 20 nm sample; (d) directly wet-etched 50 nm sample.

samples (a) and (d) display almost the same PL intensity because these two samples were not plasma etched. For sample (b) that was plasma etched of 20 nm InP cap layer, the PL intensity of the SQW is also greatly enhanced and it is 3.3 times of that of the as-grown sample.

It is an interesting issue to explore the underlying mechanism of the observed PL enhancement in the plasma etched MQW and SQW samples. The PL enhancement can be attributed to tow important factors, surface roughening caused by Ar^+ ions bombardment on sample surface and microstructural changes in the plasma-etched $InAs_{0.45}P_{0.55}/In_{0.68}Ga_{0.32}As_{0.45}P_{0.55}$ QW structures.

B. Surface roughening contribution to the PL enhancement

It is known that plasma etching can lead to surface roughening of epitaxial thin films because of ion bombardment onto sample surface. The escape probability of photons at the textured surface is increased by angular randomization, thus output of PL emission can be enhanced by the surface roughening. This effect has been used in fabricating high-brightness GaN light-emitting diodes (LEDs).[11]

The surface roughening can be measured by atomic force microscopy (AFM). We measured surface morphology of the four SQW samples: the as-grown $InAs_{0.45}P_{0.55}/InGa_{0.32}As_{0.45}P_{0.55}$ SQW sample (a), the plasma-etched 20 nm $InAs_{0.45}P_{0.55}/InGa_{0.32}As_{0.45}P_{0.55}$ SQW sample (b), the wet-etched 30 nm after plasma-etched 20 nm $InAs_{0.45}P_{0.55}/InGa_{0.32}As_{0.45}P_{0.55}$ SQW sample (c), and the directly wet-etched 50 nm $InAs_{0.45}P_{0.55}/InGa_{0.32}As_{0.45}P_{0.55}$ SQW sample (d). The lift-off of the InP capping layer in samples (c) and (d) by selectively wet etching should reveal the interface morphology as smooth as the as-grown one. Figure 3 shows four AFM images of the above four samples. The AFM image (a) for the as grown sample presents a typical MBE grown surface (very smooth) with root-mean-square (rms) surface roughness of 0.383 nm. However, after

plasma etching of 20 nm, the surface of the SQW sample becomes much rougher as shown in the image (b). Its rms roughness reaches 1.819 nm. Further, after the plasma-etched surface was removed by lift-off method, a smooth surface with rms of 0.496 nm was revealed again as shown in Fig. 3(c). Similarly, the surface of directly wet etching of the InP capping layer (without plasma etching) also reveals a similar smooth surface with rms of 0.425 nm. By comparison of the morphology changes of the four samples, it can be seen that plasma etching significantly increases the surface roughness, with rms of about five times. The surface roughening should affect the escape probability of photons from the surface.

The observed surface roughening caused by plasma etching will increase the escape probability of photons that emitted from QWs at the surface by angular randomization. We can calculate the escape probability of photons from a rough surface by using the model of Yablonovitch:[12]

$$I_{\mathrm{esc}} = 2\pi \int_0^{\theta_c} \frac{2n^2 \times I_{\mathrm{inc}}}{2\pi} \Gamma_{\mathrm{esc}}(\theta)\cos(\theta)\sin(\theta)d\theta,$$

$$T_{\mathrm{esc}}(\theta) = \left(\frac{\frac{k_s}{\rho} - \frac{k_z'}{\rho'}}{\frac{k_z}{\rho} + \frac{k_z'}{\rho'}} \right), \quad k_z = \frac{2\pi}{\lambda}\cos(\theta), \quad \begin{cases} \mathrm{TE}: \rho = 1 \\ \mathrm{TM}: \rho = \varepsilon \end{cases}. \tag{1}$$

Here, $n \sin(\theta_c) = 1$, n is the refractive index of InP and $T_{\mathrm{esc}}(\theta)$ is an angle-dependent surface transmission factor. Transverse electronic (TE) mode and transverse magnetic (TM) mode has different values of ρ. For simplicity, we substitute a weighted-average transmission factor $\bar{T}_{\mathrm{esc}}$ for the angle-dependent surface transmission factor $T_{\mathrm{esc}}(\theta)$. Then, we have $I_{\mathrm{esc}} = \bar{T}_{\mathrm{esc}} I_{\mathrm{inc}}$. For the mirror like (smooth) surface, the escape probability of photons is

$$I'_{\mathrm{esc}} = 2\int_0^{\theta_c} I_{\mathrm{inc}} \bar{T}_{\mathrm{esc}} \cos(\theta) d\theta. \tag{2}$$

The calculation by using the Yablonovitch model shows that the escape probability of photons of the plasma-etched sample is only 1.6 times of that of the as-grown sample. This value is obviously much smaller than the measured PL intensity enhancement (approximately four times) of MQW sample, which indicates that surface roughening is not the unique factor that contributes to the enhancement of PL. For the plasma-etched SQW sample, we can extract the enhancement factor due to surface roughening. As shown in Fig. 2, the PL intensity of the plasma-etched SQW sample (b) is 3.3 times of the as grown sample (a) and 1.8 times of the plasma-etched+lift-off sample (c). The difference between these two figures is, therefore, the contribution of surface roughening resulted from plasma etching. The obtained surface roughening contribution factor is 1.5 times of as grown surface. This result is consistent with the enhancement factor of 1.6 times calculated by the Yablonovitch model.

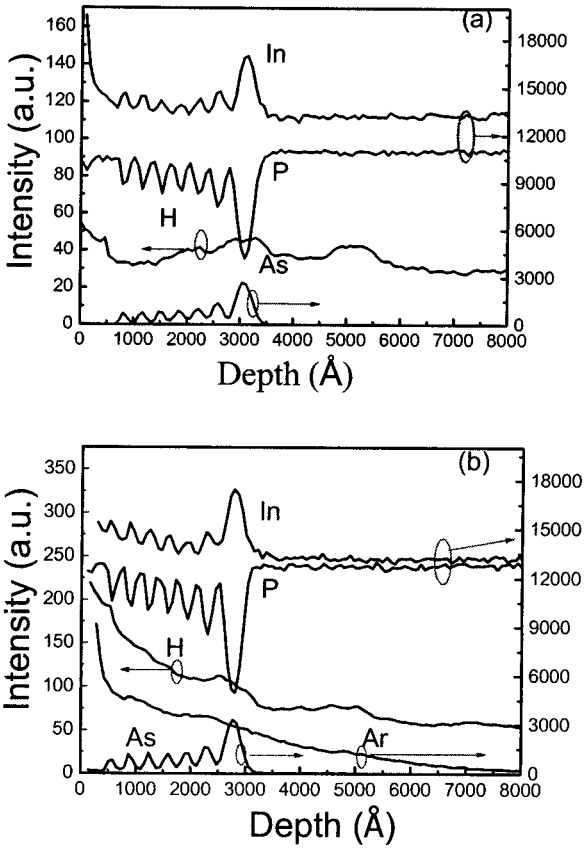

FIG. 4. SIMS measurements of $InAs_{0.45}P_{0.55}/InGa_{0.32}As_{0.45}P_{0.55}$ MQWs: (a) as-grown sample; (b) plasma-etched 45 nm sample.

C. PL enhancement due to microstructural change

The above theoretical calculation and experimental measurement result discussed in Sec. III B show that the PL enhancement factor due to surface roughening for the plasma-etched sample is only 1.6 times of that of the as-grown sample. This value is obviously much smaller than the measured PL intensity enhancement factor, which indicates that surface roughening is not the unique factor that contributes to the enhancement of PL intensity. The dominant PL enhancement factor observed in plasma-etched samples should be the result of the microstructure changes involved in plasma etching process, such as Ar^+ ions tunneling into QW structures.

To analyze microstructure changes in the plasma-etched MQWs, SIMS characterizations were performed. It is known that for different atoms the sputtering productivity of SIMS is different and the ionization rates are different as well. Here, we use arbitrary unit to present the intensity of SIMS of the as grown and plasma-etched MQW samples. Figure 4(a) plots the concentration distribution profiles for In, P, As, and H of the as grown sample. Ar signal was not detectable in the as grown sample. Figure 4(b) plots the concentration distribution profiles for In, P, As, H and Ar of the plasma-etched sample. The modulations on In, P, and As profiles in a depth range of 500–3500 Å reflect the composition variations in $InAs_{0.45}P_{0.55}/In_{0.68}Ga_{0.32}As_{0.45}P_{0.55}$ MQWs. The

noisy signals at around the sample surfaces (0–500 Å) is due to adsorbed gas disturbing to SIMS equipment, which is commonly observed in SIMS measurements. By comparison of the SIMS results, it can be seen that the concentration profiles of In, P, and As ions in the plasma-etched and as-grown samples keep almost unchanged, i.e., the intensities of In, P are ~12 000 and the intensities of As are ~1000, respectively. However, it can be seen in Fig. 4(b) that the measured profiles of In, P, and H ions in the plasma-etched sample demonstrate more significant decay characteristics from the sample surface than the as grown sample. This indicates the surface of the plasma-etched sample could be more prone to adsorb gases in air ambience, such as moisture, O_2, H_2, N_2, etc. It can be expected that the SIMS data measured inside the samples are more reliable. H ion levels in both the plasma-etched and as-grown samples are very low. In the as-grown sample, the average level of H is ~40 and after plasma etching H level is increased to ~100. The double enhancement of H level in the plasma-etched sample could be attributed to the two factors. One is more gas adsorption on the surface of the plasma-etched sample, such as moisture and H_2. The other factor may be the introduction of H in the plasma-etching process though in our plasma-etching experiments only Cl_2/Ar gases were used. However, the double enhancement of H level in the plasma-etched sample is much lower than the enhancement of Ar^+ ions shown in Fig. 4(b). It is interesting to note that the detected Ar^+ ions level in the plasma-etched MQW layers is very high (>3000), while in the as-grown sample, Ar^+ ions signal has not been detected by SIMS. We noted that in the plasma etching of the $InAs_{0.45}P_{0.55}/In_{0.68}Ga_{0.32}As_{0.45}P_{0.55}$ QW samples Ar^+ gas was used as bombardment particles and Ar^+ ions tunneled into the samples.[13] Ar^+ ions penetration into the samples is possibly the main reason of the PL enhancement observed in $InAs_{0.45}P_{0.55}/In_{0.68}Ga_{0.32}As_{0.45}P_{0.55}$ QW structures.

We also noticed that in the plasma etching of the $InAs_{0.45}P_{0.55}/In_{0.68}Ga_{0.32}As_{0.45}P_{0.55}$ QW samples Cl_2 gas was used as well. It is known that Cl only carries away the etching remnants during plasma etching. The contribution of Cl to the PL enhancement can be excluded because our further experimental result showed that a similar quantity of PL enhancement was realized even when the plasma etching was performed without Cl_2, i.e., bombarding the surface of the MQW structure with Ar^+ ions only also leads to the photoluminescence enhancement (approximately four times). It was reported that hydrogenation (H) could enhance the carrier lifetime and PL efficiency of QWs when the H concentration reaches 10^{15} ions/cm^2.[14] However, in our GSMBE growth of the $InAs_{0.45}P_{0.55}/In_{0.68}Ga_{0.32}As_{0.45}P_{0.55}$ QW structures, the concentration of H in the epitaxial layers is too low to reach this level. SIMS results shown in Fig. 4 confirmed the low H level in our samples.

From Fig. 4(b), we can see a high level of Ar^+ ions in the plasma-etched samples, and the Ar^+ ions residing in the sample exhibiting an exponential decay from the surface to the substrate. In the plasma-etching (or ICP) process, most Ar^+ ions are stopped at a few tens of nanometers below the sample surface when low ICP power is used and etching depth is small (a few tens of nanometers). The physical collision between Ar^+ ions and the lattice in the cap layer generates many physical defects around the surface region. However, high-energy Ar^+ ions can tunnel along the low-index crystal direction and penetrate deep into the sample.[13] On one hand, the tunneling process of Ar^+ ions could annihilate the grown-in defects that reside at interfaces between the barrier and well due to lattice-mismatched strain, and thus enhance the luminescence intensity.[7] On the other hand, some Ar^+ ions that tunnel along the low-index direction may substitute the lattice position of As or P in the InAsP well layer. The difference in the electronegativity between the Ar atoms and the group V atoms and the hydrostatic deformation of the lattice around the Ar sites will introduce a short-range potential. This potential allows the Ar^+ to capture an electron. The trapped electron can then bind a hole by Coulomb attraction, thus forming a bound exciton. The recombination of the bound exciton will contribute to the enhancement of PL emission in the quantum wells.[15]

However, as shown in the inset of Fig. 1, when the etching depth increases further (>50 nm) PL intensity exhibits a rapid decrease. Our further plasma-etching experiments indicate that as the etching process continues, increasingly more Ar^+ ions tunnel into the QWs, leading to the increase of density of Ar^+ ions in the QWs. These accumulated high-density Ar^+ ions form defects that are nonradiative recombination centers, and lead to the rapid decrease of photoluminescence intensity. In addition, an increased density of Ar^+ ions may also cause the disordering of the wells, which lowers the PL intensity and results in a blueshift of PL emission.

IV. CONCLUSION

Significant PL enhancement is observed of the $InAs_{0.45}P_{0.55}/In_{0.68}Ga_{0.32}As_{0.45}P_{0.55}$ SQW and MQWs after the plasma-etching process. AFM and SIMS characterizations demonstrate that the PL enhancement resulted from the microstructure change caused by Ar^+ ions tunneling into QWs and surface roughening caused by the bombardment of Ar^+ ions onto the sample surface. The combination of plasma etching and selectively wet etching the cap layer of the $InAs_{0.45}P_{0.55}/In_{0.68}Ga_{0.32}As_{0.45}P_{0.55}$ SQW revealed that the PL enhancement factors from microstructure changes and surface roughing are 1.8 and 1.5 times, respectively. The luminescence enhancement phenomenon by Ar^+ ions bombardment can be used to fabricate high-power photon-emission devices.

ACKNOWLEDGMENTS

This work has been supported by the National Key Basic Research Program of China under Grant No. 2003CB314903 and the Natural Science Foundation of China under Grant No. 10434090.

[1]H. Ichikawa, K. Inoshita, and T. Baba, Appl. Phys. Lett. **78**, 2119 (2001).
[2]J. K. Sheu, Y. K. Su, G. C. Chi, M. J. Jou, C. C. Liu, C. M. Chang, and

W. C. Hung, J. Appl. Phys. **85**, 1970 (1999).
[3]B. Li, L. Cao, and J. H. Zhao, Appl. Phys. Lett. **73**, 653 (1998).
[4]L. G. Deng, M. Rahman, and C. D. W. Wilkinson, Appl. Phys. Lett. **76**, 2871 (2000).
[5]G. Franz, J. Vac. Sci. Technol. A **19**, 762 (2001).
[6]L. S. Yu, J. D. Song, and Y. T. Lee, J. Appl. Phys. **91**, 2080 (2002).
[7]H. S. Djie, T. Mei, and J. Arokiaraj, Appl. Phys. Lett. **83**, 60 (2003).
[8]Y. Imajo, A. Kasukawa, T. Namegaya, and T. Kikuta, Appl. Phys. Lett. **61**, 2506 (1992).
[9]H. Q. Hou, A. N. Cheng, H. H. Wieder, W. S. C. Chang, and C. W. Tu, Appl. Phys. Lett. **63**, 1833 (1993).
[10]R. Y.-F. Yip *et al.*, J. Appl. Phys. **81**, 15 (1997).
[11]T. Fujii, Y. Gao, R. Sharma, E. L. Hu, S. P. DenBaars, and S. Nakamura, Appl. Phys. Lett. **84**, 855 (2004).
[12]E. Yablonovitch, J. Opt. Soc. Am. **72**, 899 (1981).
[13]M. Rahman, J. Appl. Phys. **82**, 2215 (1997).
[14]Y. L. Chang, I. H. Tan, and C. Reaves, Appl. Phys. Lett. **64**, 2658 (1994).
[15]J. C. Campbell and N. Holonyak, Jr., J. Appl. Phys. **45**, 4543 (1974).